# Synthesis of Composite ZnO-Zeolite and Its Application as Adsorbent: A Systematic Review

Jessica Veronica[1], Mamun Mollah[2], Budiman Anwar[1], Galuh Yuliani[1*)]

[1]Program Study of Chemistry, Faculty of Mathematics and Natural Science Education, Universitas Pendidikan Indonesia, Jl. Dr. Setiabudi No.229, Kota Bandung, Jawa Barat 40154 Indonesia
[2]School of Chemistry, Monash University, Clayton Campus, 3800, Australia
*Corresponding Author e-mail: galuh@upi.edu

## *Abstract*

This article aims to determine the most effective ZnO-zeolite synthesis method for use as an adsorbent. The effectiveness of the ZnO-zeolite synthesis method includes the methods of synthesis, characterization, and adsorption. This study is a literature search using Google Scholar and Science Direct with the keywords "ZnO", "zeolite", "synthesis", and "adsorption" taken from the last 10 years (2013-2023). Twenty-six articles were obtained, and selection was carried out so that 12 articles were obtained. There were 4 methods for ZnO-zeolite synthesis: (1) sol-gel, (2) impregnation, (3) coprecipitation, and (4) hydrothermal methods. The synthesis of ZnO-zeolite products was characterized using X-ray diffraction (XRD), Fourier transform infrared (FTIR) spectroscopy, and scanning electron microscopy (SEM), and their adsorption capacity was tested via UV-Vis spectroscopy. The hydrothermal synthesis method is the most effective method for the synthesis of ZnO-zeolite because it does not consume a large amount of energy, is a simple synthesis procedure, and has a large adsorption power. The resulting ZnO-zeolite has a crystal size of 1.540 μm and can adsorb up to 657.895 mg/g of the adsorbate).

**Keywords:** Adsorption, Zeolite Synthesis, ZnO-zeolite

## 1    Introduction

Zeolites are a group of aluminosilicate microporous crystalline compounds with an open three-dimensional framework consisting of $SiO_4$ and $AlO_4$ tetrahedrons connected to oxygen atoms to form intracrystal cavities and atomic-dimensional channels [1]. Zeolites have the general formula $M_{a/b}[(AlO_2)a(SiO_2)y].cH_2O$, where M represents the alkali metal or alkaline earth metal cations, b represents the valence of the alkaline earth metal cations, c is the amount of water of crystallization per unit cell, and a and y denote the total amount of $[SiO_4]^{4-}$ and $[AlO_4]^{5-}$ tetrahedra in the zeolite unit cell, respectively. The y/a ratio is in the range of 1.0 to 5.0. However, this value can change based on the structure. For example, silica-based zeolite has a value of 10.0 to 100 [2]. Zeolite has several beneficial properties such as high surface area, high thermal stability, and environmental friendliness, can increase photocatalytic efficiency; and has a uniform pore structure with straight channels to provide good adsorption properties [3,4]. Because of these properties, zeolites, such as adsorbents [5], catalysts [6], molecular sieves [7], oil refinery catalysts [8], removal of radioactive contaminants [9], $N_2O$ emission control [10], removal of heavy metals [11], soil remediation [12], and removal of polluted water [13], have been widely used in various fields of the chemical industry.

The small diameter of the zeolite formed causes the adsorption capacity to be small, so modifications are made to increase the diameter of the zeolite [14]. Currently, many researchers have begun to combine zeolite with metal oxide nanocomposites because they are considered to increase their adsorption capacity [15]. One of the metal oxide nanocomposites used for zeolite modification is zinc oxide (ZnO). ZnO is one of the hardest polar inorganic materials in semiconductor groups II-VI, with a high bond energy (60 meV) and a wide band gap (~3.2 eV)

[16]. Some of the beneficial properties of ZnO include that it is non-toxic and thermally stable, can be used as a photocatalytic pollutant such as a dye and antibacterial agent, and is environmentally friendly [17,18]. Many researchers have synthesized ZnO-zeolite and succeeded in solving the problem of wastewater, so this material is considered a promising adsorbent due to its high adsorption capacity. Tuty Emilia *et al.* (2022) succeeded in synthesizing ZnO-zeolite and degrading up to 98.24% of red dye pollutants [19]. Similarly, Georgiana Amariei *et al.* (2022) synthesized ZnO-zeolite and succeeded in degrading the antibiotic ciprofloxacin waste in less than 20 minutes at pH 4. They also demonstrated the antibacterial properties of the ZnO-zeolite material against *S. aureus* and *E. coli* [20]. However, no researcher has performed a literature review to compare the use of ZnO-zeolite synthesis methods as adsorbents.

The research literature used in this article has succeeded in producing ZnO-zeolite as an adsorbent via various methods. This scientific article aims to determine the most effective ZnO-zeolite synthesis method for use as an adsorbent. Several methods that can be used in the synthesis of ZnO-zeolite include sol-gel [19,21,22], impregnation [23–25], coprecipitation [4,26,27], and hydrothermal methods [20,28,29]. Each method used to synthesize ZnO-zeolite has different advantages, disadvantages, and results, so a review is needed to determine the most effective method. The study referred to here is a review of the cost, safety, and impact of the method on the environment.
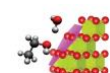
## 2 Method

Article writing was carried out using the Systematic Literature Review (SLR) method by identifying and critically assessing studies related to ZnO-zeolite for further analysis. The purpose of this study is to identify all appropriate empirical evidence to test certain hypotheses and to develop new theories. This is done to evaluate the validity and quality of findings related to ZnO-zeolite to determine its weaknesses, inconsistencies, and contradictions [30]. This journal article was analyzed by means of a literature review using Google Scholar and Science Direct searches with the keywords ZnO, zeolite, synthesis, and adsorption in the last 10 years (2013-2023). Relevant articles used as references were selected based on predetermined inclusion criteria, including the method of synthesis and application of adsorbents from ZnO-zeolite materials.

Several methods of ZnO-zeolite synthesis are analyzed in this article, namely sol-gel, impregnation, coprecipitation, and hydrothermal methods. Table 1 shows several ZnO-zeolite synthesis methods and their precursors, results, advantages, and disadvantages.

**Table 1.** Precursors, results, advantages, disadvantages, and references to the ZnO-zeolite synthesis method

| Method | Overview | | Reference |
|---|---|---|---|
| Sol-Gel | Precursors | Zinc acetate dihydrate, synthetic zeolite, isopropanol, monoethanolamine, ethanol, NaOH, fly ash, HCl | [19,21,22] |
| | Results | Cuboidal in shape with a few granular spheres and agglomerations | |
| | Advantages | Does not require special and expensive equipment | |
| | Disadvantages | Precursor costs are quite high, require a long synthesis time, and energy consumption is quite high | |
| Impregnation | Precursors | Zinc nitrate, zinc acetate dihydrate, ZnO, synthetic zeolite, HCl, ethanol, NaOH | [23–25] |
| | Results | ZnO in the form of granules is homogeneously dispersed on the surface of the zeolite | |
| | Advantages | Requires short synthesis time | |
| | Disadvantages | Requires high temperatures and a lot of tools to carry out the synthesis | |

| | | | |
|---|---|---|---|
| Co-precipitation | Precursors | Zinc acetate dihydrate, synthetic zeolite, NaOH | [4,26,27] |
| | Results | Formed a rough material surface | |
| | Advantages | The precursors used are few and relatively inexpensive | |
| | Disadvantages | Requires high temperature and long time for synthesis | |
| Hydrothermal | Precursors | Zinc acetate dihydrate, ZnCl₂, fly ash, red mud, NaOH, SiO₂, dialumunium trioxide, tetrapropylammonium, cetyltrimethyl ammonium dihydrate, ludox | [20,28,29] |
| | Results | Ferro-spherical microporous shape with several small particles scattered over the surface | |
| | Advantages | Energy consumption, simple synthesis procedure, and high reactivity | |
| | Disadvantages | Requires high cost for autoclaving and a long time for synthesis | |

## 2.1. Sol-gel method

The sol-gel method is a physicochemical process that involves the formation of an inorganic colloidal suspension (sol) and the continuous gelation of the sol in the liquid phase (gel) to form a three-dimensional network structure. The sol-gel process involves the transition of a solution system from a liquid "sol" phase to a solid "gel" phase. This method provides good particle control by increasing the porosity and decreasing the particle size [31]. Several factors affect the performance of this method, namely the hydrolysis rate, temperature, heating rate, and pH [32].

The sol-gel synthesis was started by filtering the synthetic zeolite using a 400-mesh strainer and drying it for two hours at 110ºC. After that, washing was carried out using 0.4 M hydrochloric acid for one hour, followed by washing using distilled water until the pH was neutral. The activated synthetic zeolite was then filtered and dried again in an oven at 110ºC for two hours. After that, the synthetic zeolite was mixed with zinc acetate at a ratio of 1:2 and dissolved in 80 mL of 99% ethanol. The mixture was heated at 76ºC for 2 hours and stirred continuously in a reflux flask. Then, 225 mL of sodium hydroxide was added, and the mixture was stirred again for 1 hour before it was left for 12 hours. The mixture that was allowed to stand was filtered through Whattman filter paper and the precipitate was heated in an oven at 60ºC for 24 hours to produce ZnO-zeolite. [19,21,22].

## 2.2. Impregnation Method

The impregnation method physically mixes chemical species into pores to modify the surface of a material. The impregnation methods can be divided into two types, namely wet impregnation and dry impregnation. This will depend on how the solvent is added to the absorbent surface. If the impregnation method is dry, a fixed amount of solvent is added in such a way that only the adsorbent pores are filled, whereas if the impregnation is wet, the solvent is added more than the pore volume size so that there will be an excess of chemical being dried and the loading of chemical species can be controlled [33,34].

The synthesis of ZnO-zeolite using the impregnation method begins with first filtering the synthetic zeolite using a 170-mesh filter and washing it with deionized water. After that, the zeolite was filtered and dried at 110ºC for 2 hours, and 0.4 M HCl was added before stirring using a shaker or magnetic stirrer for one hour. The zeolite was then filtered and washed again using deionized water to remove Cl⁻ ions. The zeolite residue on the filter paper was dried in an oven at 110ºC for two hours. The dried zeolite was activated with 2:1 zinc oxide solids and 100% ethanol was added. The solution was diluted with distilled water and stirred again for four hours. The homogeneous solution was exposed to ultrasonic waves for 30 minutes, dried for five hours at 120ºC, and calcined at 400ºC for two hours to obtain ZnO-zeolite [23–25].

## 2.3. Coprecipitation Method

The coprecipitation method is a method for obtaining a multicomponent material through the formation of intermediate precipitates so that a mixture of intimate components is formed during precipitation and chemical homogeneity can be maintained during the calcination process [35]. The synthesis of ZnO-zeolite using the coprecipitation method begins by dissolving the zeolite and zinc acetate in deionized water. The mixture was stirred and heated at 80°C in a reflux bottle for four hours. The homogeneous mixture was washed with deionized water and dried for five hours at 60°C. After that, 0.1 M NaOH was added until it reached a pH of 10, and the mixture was stirred for 2 hours with a magnetic stirrer, washed again with deionized water before being dried at 60°C for five hours and calcined at 450°C for two hours to obtain the ZnO-zeolite material [4,26,27].

## 2.4. Hydrothermal Method

The hydrothermal method is an inorganic synthesis method that refers to the chemical reaction occurring in water above the boiling point at different temperatures and pressures. This method involves the addition of a base as a mineralizer; generally, sodium hydroxide (NaOH); or fluoride ions ($F^-$) are added alternatively, or a structure-directing agent (SDA) is added to form the desired zeolite structure [36]. The hydrothermal method is carried out using a tool in the form of a closed vessel (autoclave) made of Teflon-coated polypropylene (PTFE) so that it requires low temperatures [37].

The synthesis of ZnO-zeolite using the hydrothermal method begins with the preparation of fly ash by washing it first with deionized water and 5 M acetic acid. After that, the washed fly ash was mixed with 1:1 zinc acetate dihydrate and dissolved in 60 mL of deionized water. The mixture was stirred continuously for 20 minutes at 500 rpm. Once homogeneous, 2 M sodium hydroxide was added until it reached pH 12, and the solution was transferred to a Teflon-lined autoclave. The solution was heated at 160°C for six hours, and the resulting product was washed five times with deionized water and dried at 80°C for 24 hours to obtain ZnO-zeolite [20,28,29].
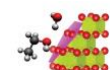
## 3    Result and Discussion

The synthesis of ZnO-zeolite has shown that it is a good and promising material because of its good adsorption ability [29]. The addition of ZnO to the zeolite significantly increased the surface area and negative charge thereby indirectly increasing the electrostatic interactions. Therefore, the adsorption capacity of ZnO-zeolite will also increase [22,29]. Several factors affect the adsorption capacity, morphology, size, and agglomeration of ZnO-zeolite, namely, the temperature used during synthesis, pH, synthesis time, and the selection of raw materials [38,39]. It is known that by increasing the temperature and synthesis time in various methods, ZnO-zeolite will be produced with a denser, more stable structure, and can provide different types of zeolite [40]. Likewise, the adsorption capacity will depend heavily on the structure and electrostatic interactions between the adsorbate used and the ZnO-zeolite material. If the adsorbate used tends to be positively charged, it is necessary to adjust the pH of the ZnO-zeolite to basic, and vice versa when the adsorbate tends to be negatively charged, ZnO-zeolite is used, which is acidic, so that electrostatic interactions will occur between the adsorbate and adsorbent. In this article, several instruments, such as XRD, FTIR, SEM, and UV-Vis, were used to further review the structure, type of zeolite formed, and adsorption capacity of ZnO-zeolite from various methods.

## 3.1. Sol-gel method

The XRD results in Figure 1 show that there are peaks for zeolite Na-A at 2θ 21.2°, 23.5°, 25.8°, 26.9°, 29.8°, and 33.8° (JCPDS 30-0222). ZnO peaks of hexagonal wurtzite structures were also found at 2θ 31.7°, 34.2°, 36.2°, 47.5°, 56.6°, 62.9°, 66.4°, 68.0°, and 69.0° which are associated with plane bounces (1 0 0), ( 0 0 2), (1 0 1), (1 0 2), (1 1 0), (1 0 3), (2 0 0), (1 1 2), and (2 0 1) (JCPDS 36-1451). In the XRD results, no impurity peaks were detected, so it can be said that the synthesized sample has high purity. The peak of the zeolite decreased with the addition of ZnO due to the interaction of ZnO with the surface of the zeolite. ZnO-zeolite with a particle size of 32.5 nm was obtained [22].

The FTIR results in Figure 2 show the presence of O-H strain vibrations due to zeolite water trapped in the pore microstructure of the zeolite framework at 3607-3200 $cm^{-1}$ and 1657 $cm^{-1}$. There are also peaks at 1200 $cm^{-1}$ and 400 $cm^{-1}$, which are attributed to Si-O-Al and Si-O bending vibrations associated with tetrahedral or alumina- and silica-oxygen bridges of the internal structure of the aluminosilicate zeolite. Weak O-H

peaks were also found in the region similar to that of Na-A zeolite (3426 cm$^{-1}$) and at 1633 cm$^{-1}$ due to the presence of water vapor absorbed from the atmosphere. The peak at 1379 cm$^{-1}$ was attributed to the -CH$_3$ group originating from the precursor, and the peak at 877 cm$^{-1}$ was attributed to the stretching peak of Zn-O. A faint peak corresponding to Si-O-Zn or Zn-O-Al was also found at 668 cm$^{-1}$ which illustrates the interaction of zeolite with ZnO on the zeolite surface. At 1032 cm$^{-1}$ there was a broadening of the peak for ZnO, which was caused by the stretching of Zn-O-ZnO. The SEM images in Figure 3 show that the morphology of the pure Na-A zeolite, which was initially cubic with a smooth surface, slowly became composed of small particles (granular spheres), which were referred to as ZnO. The level of agglomeration decreased until the addition of 1.5% ZnO; moreover, the agglomeration increased again due to excess ZnO [22].



**Figure 1.** ZnO-zeolite XRD pattern



**Figure 2.** FTIR spectra of ZnO-zeolite



**Figure 3.** SEM image of the ZnO-zeolite surface morphology

The adsorption of ZnO-zeolite increased when ZnO was loaded onto the surface of the zeolite. This is due to an increase in porosity due to the presence of micropores and mesoporous zeolite formed due to the aggregation of ZnO nanocrystals on the surface of the zeolite. The surface area of zeolite that was not combined with ZnO increased with that of zeolite combined with ZnO, from 0.40 $m^2$/g to 6.87 $m^2$/g. One possibility for the increase in surface area is the formation of a porous layer from the zeolite structure due to the presence of ZnO. The surface area can also increase when a monovalent cation is replaced with a divalent cation, in this case, one $Zn^{2+}$ cation replaces two $Na^+$ cations [22].

### 3.2. Impregnation Method

The XRD results are shown in Figure 4, which shows the peaks of zinc oxide crystals at 2θ 31.84°, 33.82°, and 36.28°. Zinc oxide disperses spontaneously onto the surface of the zeolite with the formation of monolayers or submonolayers. There was a decrease in crystallinity between zeolite without added ZnO and that with added ZnO. This is due to the increased contact between the zeolite and ZnO in the zeolite pores. Therefore, the maximum addition of ZnO is observed at 20% mass as shown in Figure 4(c) so that the resulting relative intensity does not decrease. The type of zeolite identified was Na-A zeolite. A particle size of 30.47 nm was obtained [25].
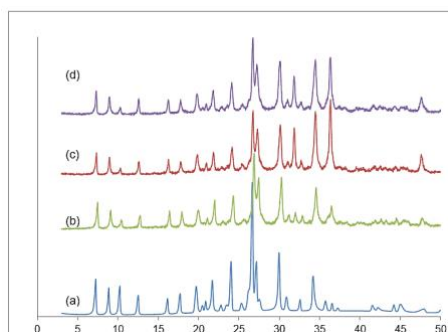


**Figure 4.** XRD patterns of (a) Zeolite, (b) 10 wt% ZnO-zeolite, (c) 20 wt% ZnO-zeolite, and (d) 30 wt% ZnO-zeolite

The FTIR results shown in Figure 5 show that there was an interaction between ZnO and the silica matrix in the 827 $cm^{-1}$ band and an increase in the intensity of the band at 419 $cm^{-1}$, which indicates the presence of a Zn-C bond. It was also found that there was an overlapping band between the ZnO band region at 600-500 $cm^{-1}$ and the zeolite band area, which is 800-400 $cm^{-1}$. There was an increase in the intensity of the 827 $cm^{-1}$ and

420 $cm^{-1}$ bands because of the increased concentration of ZnO on the surface of the zeolite. The 827 $cm^{-1}$ band, which is a Zn-Si vibrational band, also increased in intensity as the mass of the ZnO in the zeolite increased. Figure 6 shows the results of SEM analysis of ZnO-zeolite, which revealed that ZnO compounds in the form of granules are dispersed homogeneously on the surface and framework of the zeolite [25].

The adsorption property test showed that the highest adsorption capacity was obtained by adding 20% ZnO, which was 15.75 mg-S/g-adsorbent. This is because at 20 wt% ZnO-zeolite, the structural and physical properties are very good, especially for the dispersion of ZnO to support the zeolite. With the addition of excess ZnO (30 wt% ZnO-zeolite) the adsorption capacity was not too high (8.13 mg-S/g-adsorbent) due to zeolite pore blockage, damage, and the possibility of collapse of the pore structure to form aggregates. ZnO on the support surface [25].
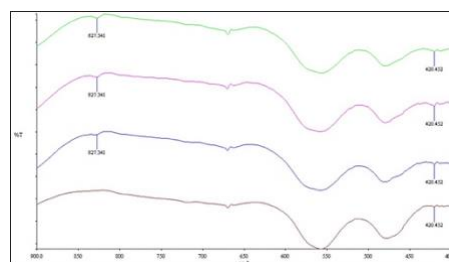


**Figure 5.** FTIR spectra of (a) zeolite, (b) 10 wt% ZnO-zeolite, (c) 20 wt% ZnO-zeolite, and (d) 30 wt% ZnO-zeolite
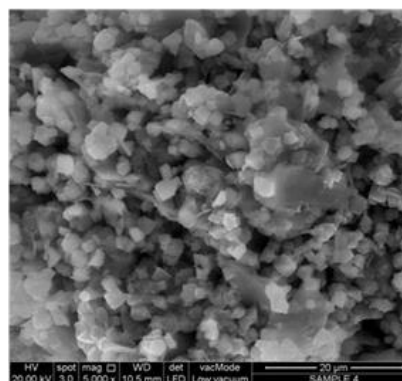


**Figure 6.** SEM image of the ZnO-zeolite surface morphology

### 3.3. Co-Precipitation Method

The XRD results are shown in Figure 7, which shows the suitability of the clinoptilolite zeolite peaks on 2θ 9.9°, 11.2°, 17.3°, 19.1°, 22.4°, 26.3°, and 30.0° (JCPDS 25-1349). Heulandite zeolite peaks were also found on heulandite zeolite

peaks 2θ 9.9°, 11.2°, 17.3°, 19.1°, 22.4°, 28.1°, and 30.0° (JCPDS 53-1176), as well as on mordenite zeolite peaks at 2θ 9.9°, 13.5°, 19.6°, 22.4°, 25.6°, and 27.7° (JCPDS 29-1257). No characteristic peaks were found for ZnO because the amount of ZnO present in the material was too small (< 9%). The obtained surface area for ZnO-zeolite was 31.835 m$^2$/g, and the particle size was 399 nm [27].
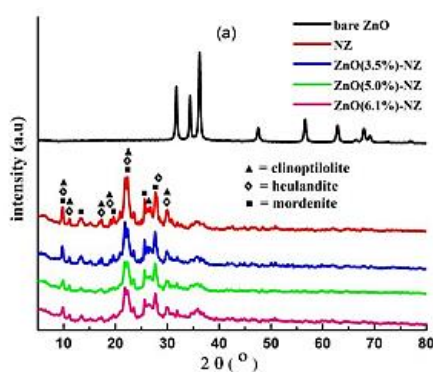


**Figure 7.** ZnO-zeolite XRD pattern

The FTIR results in Figure 8 shows the presence of the O-H band with a strain vibration at 3700-3000 cm$^{-1}$, which corresponds to ≡Al-OH-Si≡ and adsorbed water molecules. The O-H bending vibration of the absorbed water molecule is at a band length of 1636 cm$^{-1}$. The 1049 cm$^{-1}$ band corresponds to the asymmetric stretching vibrations of Si(Al)-O in zeolite, and the 795 cm$^{-1}$ band corresponds to the symmetric stretching vibrations of Si(Al)-O. The band at 471 cm$^{-1}$ corresponds to the bending vibration of Si(Al)-O. In addition, there is an absorption peak at 594 cm$^{-1}$, indicating the presence of a double-ring outer zeolite bond from the heulandite phase and ZnO stretching vibrations at a bond length of 400-500 cm$^{-1}$. The results of the SEM-EDS analysis of the ZnO-zeolite material are shown in Figure 9. A rough surface of the material is formed as a result of the formation of ZnO groups on the surface of the zeolite [27].

In testing the adsorption properties of ZnO-zeolite, it was found that the presence of ZnO in the zeolite structure causes the material size to decrease so that the surface area will be much larger to contact the adsorbate so that it will increase its adsorption capacity. Another factor that increases the adsorption capacity is the electronegativity of the zeolite. In addition, exposure to ultraviolet light is also considered efficient for degrading dyes due to the distortion of the chromophore groups in the dye due to

photodecomposition through the formation of radical species. The radical species in question is the hydroxyl radical (•OH) resulting from the photolysis of water and ZnO. Therefore, the greater the amount of ZnO, the more radicals will be formed so that more dye will be degraded. Even so, a dose of ZnO that is too high can also reduce the penetration of photons into the solution so that it will be less effective in degrading it. The obtained ZnO-zeolite can adsorb up to 90% of the adsorbate [27].
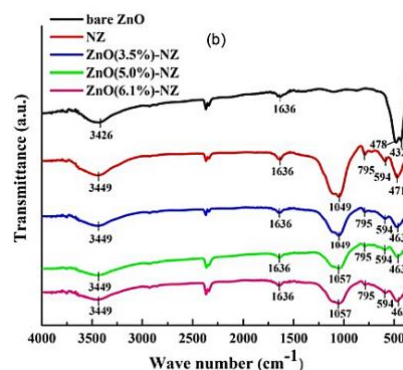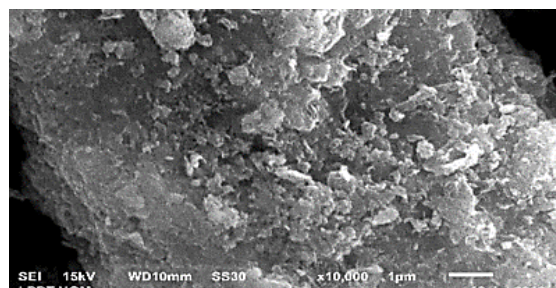


**Figure 8.** FTIR Spectra of ZnO-zeolite



**Figure 9.** SEM image of the ZnO-zeolite surface morphology

### 3.4. Hydrothermal Method

The XRD results shown in Figure 10(a) correspond to the mineralogical compositions of quartz-Q (JCPDS: 00-046-1045) and mullite-M (01-079-1275). After activation using zinc acetate dihydrate and sodium hydroxide, a new peak was found that corresponds to the peaks of the cancrinite zeolite (ICSD: 20334) and analcime zeolite (JCPDS: 01-076-0143, Supelano et al., 2020). In addition, peaks at 2θ = 31.8° and 34.4° were also obtained, which correspond to the (1 0 0) and (0 0 2) reflection planes of the ZnO hexagonal wurtzite structure (JCPDS: 89-13971, Rodwihok, Wongratanaphisan, et al., 2019). A sodium aluminosilicate diffraction peak was also found, indicating that zeolization had occurred and that a peak shift had occurred (1 0 1) from

36.2° to 38.44° so that Zn atoms were known to have undergone substitution causing zeolite cancrinite and analcime structures. Figure 10(e). is the result of characterization from FESEM with elemental mapping using EDS from Si, Al, O, Na, and Zn content. The morphological results showed that the ZnO-zeolite was in the form of ferro-spherical micropores with several small particles

scattered throughout the surface with an average particle size of 1.540 μm. EDS elemental mapping analysis also provided evidence that all the elements were homogeneously distributed and that some oxides were present in all the samples [29].
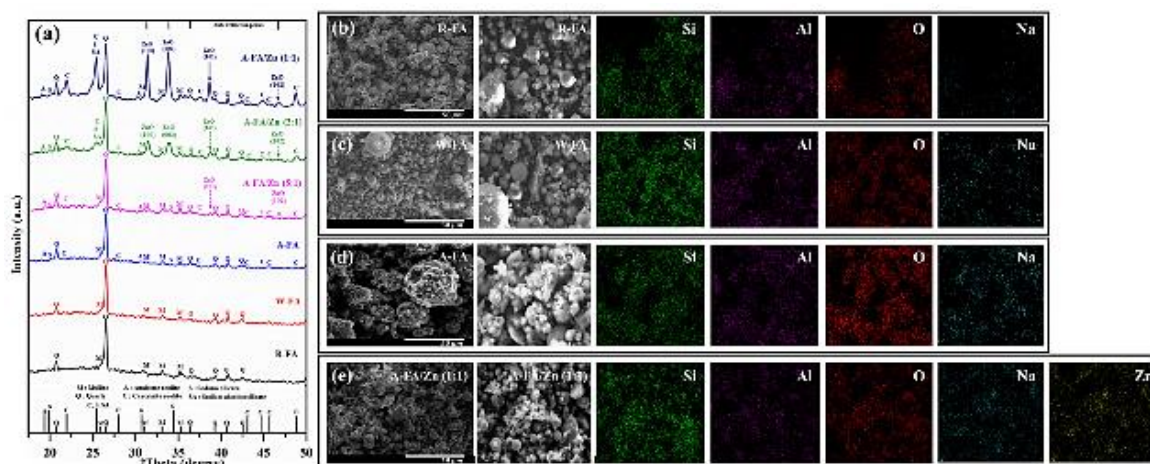


**Figure 10. (a)** ZnO-zeolite XRD pattern; Surface morphology of FESEM with EDS **(b)** fly ash, **(c)** washed fly ash, **(d)** zeolite without ZnO, **(e)** ZnO-zeolite

The FTIR characterization results in Figure 11 show that there is a broad absorption band at 3300-3600 $cm^{-1}$ and a small peak at approximately 1650-2000 $cm^{-1}$, which corresponds to the stretching vibrations of each O-H and C=O group. In addition, bands at 1647 $cm^{-1}$ were also found, which were attributed to the bending vibrations of silanol groups (Si-OH); peaks at 1097, 974, 754 and 678 $cm^{-1}$ which were attributed to the asymmetric stretching vibrations of Si-O-Si; the stretching vibrations of symmetric and asymmetric internal tetrahedral groups (O-T-O; T = Si/Al in $TO_4$ units); and Si-O-Al symmetric strain vibrations. A small peak was also found at 565 $cm^{-1}$ which was the peak of the Zn-O bond strain, indicating that ZnO had formed on the ZnO-zeolite surface [29].

In testing the adsorption properties of ZnO-zeolite, it was found that electrostatic interactions play an important role in increasing the adsorption capacity. The results of the analysis using the Zetasizer instrument showed a large surface charge of ZnO-zeolite (-24.32 eV) compared to that of pure fly ash (-13.40 eV) and zeolite without the addition of ZnO (-19.85 eV). This is due to the presence of OH groups on the adsorbent surface so that because of electrostatic repulsion, the
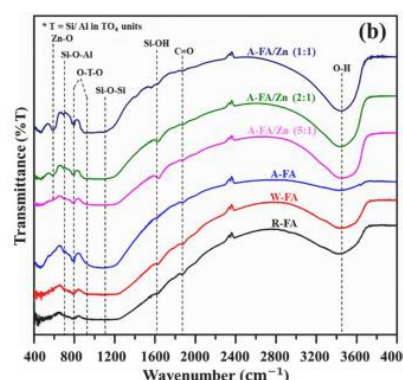
adsorbent surface, which has a high negative charge, will provide a greater attractive force for adsorption on positive charges. In this case, it is known that the increase in the electrostatic interaction of zeolization and the formation of ZnO plays an important role in increasing the adsorption capacity of ZnO-zeolite. UV-Vis analysis revealed that ZnO-zeolite adsorbs dyes according to the Koble-Corrigan isotherm model with pseudo-second-order adsorption kinetics of 657.895 mg/g [29].



**Figure 11**. FTIR Spectra of ZnO-zeolite

## 4 Conclusion

In the manufacture of ZnO-zeolite, several methods can be used to synthesize ZnO-zeolite, namely, sol-gel synthesis, impregnation, coprecipitation, and hydrothermal methods. Among these methods, the most effective method for synthesizing ZnO-zeolite is the hydrothermal method. This is because the hydrothermal method consumes a large amount of energy, the synthesis procedure is simple, and the hydrothermal process has a large adsorption power. The resulting ZnO-zeolite, which has a nonagglomerated crystal size of 1.540 µm and can adsorb up to 657.895 mg/g of adsorbate. In the adsorption ability test, it is also known that the charge carried by ZnO increases the electrostatic interaction between the ZnO-zeolite material and the adsorbate.

## References

[1] Azizi-Lalabadi, M., Ehsani, A., Divband, B. and Alizadeh-Sani, M. 2019. Antimicrobial activity of Titanium dioxide and Zinc oxide nanoparticles supported in 4A zeolite and evaluation the morphological characteristic. *Scientific Reports*, 9 (1) 17439. 10.1038/s41598-019-54025-0

[2] Lakiss, L., Gilson, J.P., Valtchev, V., Mintova, S., Vicente, A., Vimont, A. et al. 2020. Zeolites in a good shape: Catalyst forming by extrusion modifies their performances. *Microporous and Mesoporous Materials*, 299 110114. 10.1016/j.micromeso.2020.110114

[3] Algieri, C. and Drioli, E. 2022. Zeolite membranes: Synthesis and applications. *Separation and Purification Technology*, 278 119295. 10.1016/j.seppur.2021.119295

[4] Alswata, A.A., Ahmad, M. Bin, Al-Hada, N.M., Kamari, H.M., Hussein, M.Z. Bin and Ibrahim, N.A. 2017. Preparation of Zeolite/Zinc Oxide Nanocomposites for toxic metals removal from water. *Results in Physics*, 7 723–31. 10.1016/j.rinp.2017.01.036

[5] Zhang, Y., Chen, Y., Kang, W., Han, H., Song, H., Zhang, C. et al. 2020. Excellent adsorption of Zn(II) using NaP zeolite adsorbent synthesized from coal fly ash via stage treatment. *Journal of Cleaner Production*, 258 120736. 10.1016/j.jclepro.2020.120736

[6] Liang, J., Shan, G. and Sun, Y. 2021. Catalytic fast pyrolysis of lignocellulosic biomass: Critical role of zeolite catalysts. *Renewable and Sustainable Energy Reviews*, 139 110707. 10.1016/j.rser.2021.110707

[7] Chen, L., Deng, Y., Han, W., Jiaqiang, E., Wang, C., Han, D. et al. 2022. Effects of zeolite molecular sieve on the hydrocarbon adsorbent and diffusion performance of gasoline engine during cold start. *Fuel*, 310 122427. 10.1016/j.fuel.2021.122427

[8] Naranov, E.R., Dement'ev, K.I., Gerzeliev, I.M., Kolesnichenko, N. V., Roldugina, E.A. and Maksimov, A.L. 2019. The role of zeolite catalysis in modern petroleum refining: Contribution from domestic technologies. *Petroleum Chemistry*, 59 (3) 247–61. 10.1134/S0965544119030101

[9] Kwon, S., Kim, C., Han, E., Lee, H., Cho, H.S. and Choi, M. 2021. Relationship between zeolite structure and capture capability for radioactive cesium and strontium. *Journal of Hazardous Materials*, 408 124419. 10.1016/j.jhazmat.2020.124419

[10] Li, D., Manu, M.K., Varjani, S. and Wong, J.W.C. 2022. Mitigation of NH3 and N2O emissions during food waste digestate composting at C/N ratio 15 using zeolite amendment. *Bioresource Technology*, 359 127465. 10.1016/j.biortech.2022.127465

[11] Hong, M., Yu, L., Wang, Y., Zhang, J., Chen, Z., Dong, L. et al. 2019. Heavy metal adsorption with zeolites: The role of hierarchical pore architecture. *Chemical Engineering Journal*, 359 363–72. 10.1016/j.cej.2018.11.087

[12] Belviso, C. 2020. Zeolite for potential toxic metal uptake from contaminated soil: A brief review. *Processes*, 8 (7) 820. 10.3390/pr8070820

[13] Mancinelli, M., Arfè, A., Martucci, A., Pasti, L., Chenet, T., Sarti, E. et al. 2020. Evaluation for the removal efficiency of vocs and heavy metals by zeolites-based materials in the wastewater: A case study in the tito scalo industrial area. *Processes*, 8 (11) 1–14. 10.3390/pr8111519

[14] Król, M. 2020. Natural vs. synthetic zeolites. *Crystals*, 10 (7) 1–8. 10.3390/cryst10070622

[15] YANG, Y., Mandizadeh, S., ZHANG, H. and Salavati-Niasari, M. 2021. The role of ZnO in reactive desulfurization of diesel over ZnO@Zeolite Y: Classification, preparation, and evaluation. *Separation and Purification Technology*, 256 117784. 10.1016/j.seppur.2020.117784

[16] Saravanan, R., Thirumal, E., Gupta, V.K., Narayanan, V. and Stephen, A. 2013. The photocatalytic activity of ZnO prepared by simple thermal decomposition method at various temperatures. *Journal of Molecular*

*Liquids*, 177 394–401. 10.1016/j.molliq.2012.10.018

[17] Cruz, G.J.F., Gómez, M.M., Solis, J.L., Rimaycuna, J., Solis, R.L., Cruz, J.F. et al. 2017. Composites of ZnO nanoparticles and biomass based activated carbon: Adsorption, photocatalytic and antibacterial capacities. *Water Science and Technology*, 2017 (2) 492–508. 10.2166/wst.2018.176

[18] He, X., Yang, D.P., Zhang, X., Liu, M., Kang, Z., Lin, C. et al. 2019. Waste eggshell membrane-templated CuO-ZnO nanocomposites with enhanced adsorption, catalysis and antibacterial properties for water purification. *Chemical Engineering Journal*, 369 621–33. 10.1016/j.cej.2019.03.047

[19] Agustina, T.E., Gayatri, R., Bahrin, D., Moeksin, R. and Gustini. 2022. Zno-zeolite nanocomposite application for photocatalytic degradation of procion red and its adsorption isotherm. *Acta Polytechnica*, 62 (2) 238–47. 10.14311/AP.2022.62.0238

[20] Amariei, G., Valenzuela, L., Iglesias-Juez, A., Rosal, R. and Visa, M. 2022. ZnO-functionalized fly-ash based zeolite for ciprofloxacin antibiotic degradation and pathogen inactivation. *Journal of Environmental Chemical Engineering*, 10 (3) 107603. 10.1016/j.jece.2022.107603

[21] Gayatri, R., Agustina, T.E., Bahrin, D., Moeksin, R. and Gustini, G. 2020. Preparation and characterization of ZnO-Zeolite nanocomposite for photocatalytic degradation by ultraviolet light. *Journal of Ecological Engineering*, 22 (2) 178–86. 10.12911/22998993/131031

[22] Munguti, L.K., Dejene, F.B. and Muthee, D.K. 2023. High photodegradation performance of ZnO nanoparticles supported on porous Zeolite Na-A: Effects of ZnO loading. *Materials Chemistry and Physics*, 295 127063. 10.1016/j.matchemphys.2022.127063

[23] Salam, A., Agustina, T.E. and Mohadi, R. 2018. Photocatalytic degradation of procion red synthetic dye using ZnO-Zeolite composites. *International Journal of Scientific & Technology Research*, 7 (8) 54–9.

[24] Sacco, O., Vaiano, V. and Matarangolo, M. 2018. ZnO supported on zeolite pellets as efficient catalytic system for the removal of caffeine by adsorption and photocatalysis. *Separation and Purification Technology*, 193 303–10. 10.1016/j.seppur.2017.10.056

[25] Abdullah, A.H., Mat, R., Somderam, S., Abd Aziz, A.S. and Mohamed, A. 2018. Hydrogen sulfide adsorption by zinc oxide-impregnated zeolite (synthesized from Malaysian kaolin) for biogas desulfurization. *Journal of Industrial and Engineering Chemistry*, 65 334–42. 10.1016/j.jiec.2018.05.003

[26] Agustina, T.E., Prajawita, A.U. and Sinaga, S.A.S. 2020. The effect of pH on Synthesis of ZnO-Natural zeolite nanocomposite by Co-precipitation method. *IOP Conference Series: Materials Science and Engineering*, 845 (1) 012049. 10.1088/1757-899X/845/1/012049

[27] Diantariani, N.P., Kartini, I, Kuncaka, A. and Wahyuni, E.T. 2020. Zno incorporated on natural zeolite for photodegradation of methylene blue. *Rasayan Journal of Chemistry*, 13 (1) 747–56. 10.31788/RJC.2020.1315597

[28] Tehubijuluw, H., Subagyo, R., Kusumawati, Y. and Prasetyoko, D. 2022. The impregnation of ZnO onto ZSM-5 derived from red mud for photocatalytic degradation of methylene blue. *Sustainable Environment Research*, 32 (1) 4. 10.1186/s42834-021-00113-8

[29] Rodwihok, C., Suwannakeaw, M., Charoensri, K., Wongratanaphisan, D., Woon Woo, S. and Kim, H.S. 2021. Alkali/zinc-activated fly ash nanocomposites for dye removal and antibacterial applications. *Bioresource Technology*, 331 125060. 10.1016/j.biortech.2021.125060

[30] Xiao, Y. and Watson, M. 2019. Guidance on conducting a systematic literature review. *Journal of Planning Education and Research*, 39 (1) 93–112. 10.1177/0739456X17723971

[31] Brinker, C.J. and Scherer, G.W. 2013. Sol-Gel Science: The Physics and Chemistry of Sol-Gel Processing. Sol-Gel Science: The Physics and Chemistry of Sol-Gel Processing. Elsevier. 10.1016/C2009-0-22386-5

[32] Khaleque, A., Alam, M.M., Hoque, M., Mondal, S., Haider, J. Bin, Xu, B. et al. 2020. Zeolite synthesis from low-cost materials and environmental applications: A review. *Environmental Advances*, 2 100019. 10.1016/j.envadv.2020.100019

[33] Singh, L., Rekha, P. and Chand, S. 2016. Cu-impregnated zeolite Y as highly active and stable heterogeneous Fenton-like catalyst for degradation of Congo red dye. *Separation*
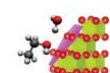
*and Purification Technology*, 170 321–36. 10.1016/j.seppur.2016.06.059

[34] Girish, C.R. 2018. Various impregnation methods used for the surface modification of the adsorbent: A review. *International Journal of Engineering and Technology(UAE)*, 7 (4.7 Special Issue 7) 330–4. 10.14419/ijet.v7i4.7.20571

[35] Bajaj, N.S. and Joshi, R.A. 2021. Energy materials: Synthesis and characterization techniques. *Energy Materials: Fundamentals to Applications*, Elsevier. p. 61–82. 10.1016/B978-0-12-823710-6.00019-4

[36] Mallada, R. 2014. Hydrothermal Synthesis of Zeolite. *Encyclopedia of Membranes*, Springer Berlin Heidelberg, Berlin, Heidelberg. p. 1–2. 10.1007/978-3-642-40872-4_953-1

[37] Sangeetha, C. and Baskar, P. 2016. Zeolite and its potential uses in agriculture : A critical review. *Agricultural Reviews*, 37 (2) 101–8. 10.18805/ar.v0iof.9627

[38] Muhammad, S., Machdar, I. and Saputra, E. 2014. Hydrothermal Synthesis of Nanocrystalline Zeolite using Clear Solution. *The 5th Sriwijaya International Seminar on Energy and Environmental Science & Technology*, Palembang. p. 80–6.

[39] Cruz, T.J.T., Melo, M.I.S. and Pergher, S. 2020. Optimization of parameters and methodology for the synthesis of LTA-type zeolite using light coal ash. *Applied Sciences*, 10 (20) 7332. 10.3390/app10207332

[40] Paramitha, T. 2020. Conversion of Coal Fly Ash to Zeolite by Alkaline Fusion-Hydrothermal Method: A Review. *Proceedings of the International Seminar of Science and Applied Technology (ISSAT 2020)*, Atlantis Press, Paris, France. 10.2991/aer.k.201221.067

[41] Supelano, G.I., Gómez Cuaspud, J.A., Moreno-Aldana, L.C., Ortiz, C., Trujillo, C.A., Palacio, C.A. et al. 2020. Synthesis of magnetic zeolites from recycled fly ash for adsorption of methylene blue. *Fuel*, 263 116800. 10.1016/j.fuel.2019.116800

[42] Rodwihok, C., Wongratanaphisan, D., Thi Ngo, Y.L., Khandelwal, M., Hur, S.H. and Chung, J.S. 2019. Effect of GO additive in ZnO/rGO nanocomposites with enhanced photosensitivity and photocatalytic activity. *Nanomaterials*, 9 (1441) 2–18. 10.3390/nano9101441